Structure and Silver Ion Transport in $AgI-Ag_2MoO_4$ Glasses: A Molecular Dynamics Study†

A. Karthikeyan and K. J. Rao*

Solid State and Structural Chemistry Unit, Indian Institute of Science, Bangalore 560 012, India

Received: July 15, 1996; In Final Form: November 15, 1996⊗

The structure and dynamics of silver ion conducting $AgI-Ag_2MoO_4$ glasses have been simulated by molecular dynamics simulation over a wide range of compositions. Formation of silver iodide like aggregates have been identified only in the AgI rich glasses. Increase in silver ion conductivity with an increase in AgI content in the glass is seen as in experiments. The dynamics of ion transport suggests that Ag^+ ion transport occurs largely through paths connected by silver ion sites of mixed iodide−oxide coordination. The Van Hove correlation functions indicate that Ag^+ ions prefer migration along the pathways formed with connected sites of similar coordination.

1. Introduction

Silver-based glasses have been found to exhibit excellent ionic conductivity even at ambient temperatures.[1−7] Such fast ionic conduction (FIC) glasses have therefore been considered as potential candidates for solid state microbatteries and other device applications.[4,8] Various silver-based FIC glasses have been synthesized with the general formula $AgI-Ag_2O-M_xO_y$ (M = Mo, B, P, V, etc., in ternary systems) or $AgI-Ag_zM_xO_y$ (M = Mo, Se, etc., in pseudobinary systems). All these glasses have silver ion conductivity on the order of 0.01 S cm^{-1}, and the conductivity strongly depends on the concentration of AgI. To understand the origin of such high silver ion conductivity of these glasses, structural information at the molecular level is needed. Several transport models have been proposed based on hypothetical microstructure with little experimental support,[1,9−11] and a satisfactory transport theory supported by clear experimental evidence has not been achieved so far.

The presence of tetrahedrally coordinated molybdenum has been noted in a number of studies such as infrared spectroscopy, XANES, and EXAFS in $AgI-Ag_2O-MoO_3$ glasses.[5,12] Similar tetrahedral anion framework has been reported in other silver ion conducting glasses such as $AgI-Ag_2O-P_2O_5$ also. The network structure present in such glasses is not modified by the addition of silver halide.[13] Minami[10] postulated the existence of two distinct populations of silver ions in these glasses, namely, the mobile silver ions associated with AgI, which are responsible for high ionic conduction, and the immobile silver ions linked with oxy-anionic species in the glasses. The ion exchange experiments and acoustic attenuation studies have supported the possible presence of nonequivalent Ag^+ sites.[14,15] However, the NMR investigations by Martin et al.[16] contradict the concept of two types of Ag^+ ions. They could detect distinct Ag^+ ion populations only at low temperatures. Further, the ^{109}Ag chemical shift measurements by Villa et al.[17] suggests that all Ag^+ ions are structurally equivalent. Recently the far infrared study by Kamitsos et al.[18] suggested that silver ions actually occupy several different types of sites, at least two types of "oxidic" and one "iodidic" site.

The high ionic conductivity in AgI-containing glasses is often attributed to the presence of frozen α-AgI structure in glasses. Shiraldi et al.[19] argued that the supercooled α-AgI phase is somehow stabilized by the "hard" oxy-anionic glass framework. Malugani et al.[20] found that in MI_2-AgPO_3 (M = Cd, Hg, Pb), the introduction of Ag^+ in the form of AgI rather than as $AgPO_3$ caused a rapid increase in the conductivity. The authors attribute the conductivity rise to the formation of AgI due to the exchange of Cd^{2+} or Pb^{2+} with Ag^+ ions and formation of α-AgI-like structures in glasses. Further, in $AgI-AgPO_3$ glasses, microheterogeneities have been identified by SANS by Tachez et al.[3,6] However, Brillouin scattering and SANS experiments on $(MX)_x-(M_2O-nB_2O_3)_{1-x}$ (MX = LiCl, AgI) glasses by Borjesson et al.[21] have shown the absence of any significant scattering from inhomogeneities. Misinu et al.[22,23] on the basis of their diffractometric and spectroscopic studies, also consider that the model based on α-AgI-like clusters does not account for their experimental observations in $AgX-Ag_2O-B_2O_3$ and $AgX-Ag_2O-P_2O_5$ (X = I, Br, Cl) glasses. Further, the X-ray[24] and EXAFS[25] studies provide evidence against the α-AgI cluster hypothesis. However, Tatsumisago et al.[26,27] have reported the possibility of quenching α-AgI structures of high ionic conductivity directly from high temperatures in otherwise difficult glass forming AgI rich compositions.

The ionic conduction behavior in glasses in general has been addressed using a cluster-tissue model[28,29] in which the structure of the glass is visualized as being composed of clusters of slightly higher density and positional ordering of constituent atoms connected by a tissue material of lower density and greater disorder. The conductivity in clusters is considered as higher than in tissue, and conductivity enhancement is explained through the increased interconnection between highly conducting clusters, which provides a continuous path for the ion migration. High-pressure studies carried out previously in this laboratory[30,31] on $AgI-Ag_2O-MoO_3$ agree well with this cluster model. However according to Ingram et al.,[11,32] preferred pathways for migration of silver ions lie well within the amorphous tissue region. Cluster formation has been evidenced in HREM[33] of $AgI-Ag_2MoO_4$ glasses, in neutron scattering[6,34] and in Raman scattering[35] experiments. Recent neutron scattering experiments by Dianaux et al.[36] on $AgPO_3-AgBr/AgI$ have supported the formation of clusters as Ag^+ and I^- ion aggregates. However these clusters are much larger in size than can be examined using computer modeling.

† Communication number 1159 from Solid State and Structural Chemistry Unit, Indian Institute of Science, Bangalore, India.

* Corresponding author. Tel: 91-80-3344411, ext. 2583. Telefax: 91-80-3341683. E-mail: kjrao@sscu.iisc.ernet.in.

⊗ Abstract published in *Advance ACS Abstracts,* March 1, 1997.

S1089-5647(96)02100-1 CCC: $14.00

Computer simulation studies have been reported in some Ag^+ ion conducting glasses. Molecular dynamics simulations of $AgI-Ag_2O-B_2O_3$ glasses by M. C. Abramo et al.[37,38] have indicated the possibility of medium-range ordering due to formation of AgI clusters, which coexist with the B_2O_3 network. But the structural details of clustered regions and dynamics of the ions have not been discussed in their simulation work. Most recently, J. D. Wicks et al.[39] have studied the structure and ionic conduction in $AgI-AgPO_3$ glasses, and they find strong evidence for the formation clusters of Ag and I with correlation lengths of up to 20−30 Å. The reverse Monte Carlo simulations by the same authors indicated increase in the free volume available for Ag^+ ion motion, which therefore leads to enhancement in ionic conductivity.[39]

Thus, there is a clear need for understanding the microstructure and the transport mechanism in silver ion based FIC glasses. Important questions that have to be addressed regarding structure in this class of materials are (i) is there any cluster formation and, if so, are the local atomic correlations within the clusters α-AgI-like, and (ii) how are the silver ions coordinated to the oxy-anionic glass units? Similar questions that should be addressed regarding the transport mechanism are (i) are all silver ions equally mobile irrespective of the local environments, and (ii) are there preferred pathways for silver ion motion? These questions regarding structure and conduction mechanisms can be effectively examined using molecular dynamics (MD). Born−Mayer−Huggins (BMH) pair potential is often used in MD simulations of ionic glasses.[40,41] Numerous MD simulations in earlier works from this laboratory[42−46] on glasses such as $PbO-SiO_2$, ZrO_2-SiO_2, and mixed alkali silicate and sulfate glasses have been successfully carried out using BMH potentials. The results obtained from simulations were found to agree very well with the experimental observations. Also, Abramo et al.[37,38] have demonstrated the effectiveness of using BMH potentials in elucidating the various pair correlations functions in the case of $AgI-Ag_2O-B_2O_3$ glasses. In this background we have now performed the MD simulations of xAgI−$(100-x)Ag_2MoO_4$ glasses of varying AgI contents (x = 20−80 in steps of 20) using the BMH potential. The methodology is presented in the following section, and the results are presented and discussed in the later sections.

2. Methodology

The system used in the present simulation work consists of silver and iodide ions along with discrete and rigid tetrahedral molybdate MoO_4^{2-} ions. The presence of such discrete tetrahedral MoO_4^{2-} units is well established by a number of experiments in $AgI-Ag_2MoO_4$ glasses by Minami et al.[10] and Rao et al.[12] The molecular dynamics simulation was performed on a system of N particles in the microcanonical (NEV) ensemble. Initial configuration of the system was generated inside a cubic box by fixing the coordinates randomly (coordinate of the center of mass was generated for MoO_4^{2-} ions). The volume of the simulation box was fixed such that it is consistent with the real density of the $AgI-Ag_2MoO_4$ glass. The interactions were calculated using the Born−Mayer−Huggins potential[43,46] V_{ij},

$$V_{ij} = (Z_iZ_j/r_{ij}) + A_{ij}\exp[(\sigma_{ij} - r_{ij})/\rho_{ij}] \qquad (1)$$

where $A_{ij} = b_{ij}[1 + Z_i/n_i + Z_j/n_j]$ (Z_i, Z_j are charges and n_i, n_j are the number of valence-shell electrons in the ions). The first term (Coulomb energy) has been calculated using the Ewald sum which contains real and reciprocal space contributions.[43] The various interaction parameters used in the present simulations are listed in Table 1. There is no data available to fix the charges on Mo and O atoms on MoO_4^{2-} ions. However work on sulfates and silicates shows clear indications that charges on O and Mo have to be different and much lower than the formal charges. Charges calculated on the basis of electronegativity equalization principle indicate that charges on O (−0.64) and Mo (0.56) are much lower than −2 and +6, respectively. We have therefore, on the basis of a few quick and approximate initial simulations, fixed the charge on Mo and O as indicated in Table 1. Periodic boundary conditions were applied to simulate the infinite system. The fifth-order Gear predictor−corrector algorithm[47] was used to integrate the equations of motion with a time step 1 fs. The translation and rotation of the MoO_4^{2-} groups were considered at each time step. The orientation of the MoO_4^{2-} units was specified by quaternions (q_0, q_1, q_2, q_3).[47] Quaternions here are coordinates of tetrahedral anions with fixed relations among constituent atoms. (The center of mass of such ions lies on the central atom, which is subjected to dynamics, and translations of all other atoms are automatically carried out by movement of the center of mass. Rotational motion changes quaternions except the coordinates of the center of mass.) The initial quaternion parameters of all MoO_4^{2-} units were taken as (1, 0, 0, 0). The Mo−O distance in the tetrahedron was held constant at 1.75 Å and was taken from the Mo−O distance in the MoO_4^{2-} tetrahedral units of crystalline Mo_4O_{11}.[48] Initial simulation was performed at 5000 K by choosing appropriate velocities. The system was then cooled to 3000 K and then to 1000 K at a rate of 1 K/fs. Further cooling was done at the rate of 0.1 K/fs to 700 K and to 300 K. The densities at high temperatures were chosen so as to keep the pressure zero, and at room temperature the real experimental density[49] values were used. The pressures were also satisfactorily low (less than 5 kbar). The compositions of the glasses studied, density, size of the computational cell, etc., are listed in Table 2. At each temperature, the system was equilibrated for more than 40 ps and the data were stored for another 60 ps. Various structural and dynamical properties were obtained from these stored data.

TABLE 1: Potential Parameters Used in BMH Potential[a]

	Ag	I	Mo	O
Z_i (e units)	+1.0	−1.0	+1.2	−0.8
σ (Å)	2.32	3.36	1.24	2.44

[a] Common values of ρ_{ij} = 0.29 Å and b = 0.338 × 10^{-19} J have been employed. Also $\sigma_{ij} = (\sigma_i + \sigma_j)/2$ and $\sigma_{ii} = \sigma$.

TABLE 2: Compositions, Density, and Size of the Simulation Cell

	glass			
parameters	SM20	SM40	SM60	SM80
number of molecules				
AgI	14	32	60	108
Ag_2MoO_4	56	48	40	27
N	420	400	400	405
density (g/cm^3)	6.0	6.1	6.2	6.3
box length (Å)	18.882	19.087	19.830	21.072

3. Results and Discussion

Four compositions of the glass in the system x%AgI−$(100-x)$%Ag_2MoO_4 have been studied. These compositions cover nearly entirely the known experimental glass compositions. These compositions are named SM20, etc., (where SM is silver molybdate and the number is percentage of AgI). In all these compositions the total cohesive energy of the system was found to be constant to approximately one part in 10^5. A

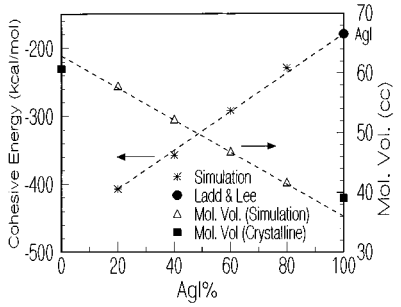

Figure 1. Plot of cohesive energies and molar volumes of the system at 300 K as a function of AgI content in the glass. The energy of pure β-AgI was obtained from Ladd and Lee.[50]

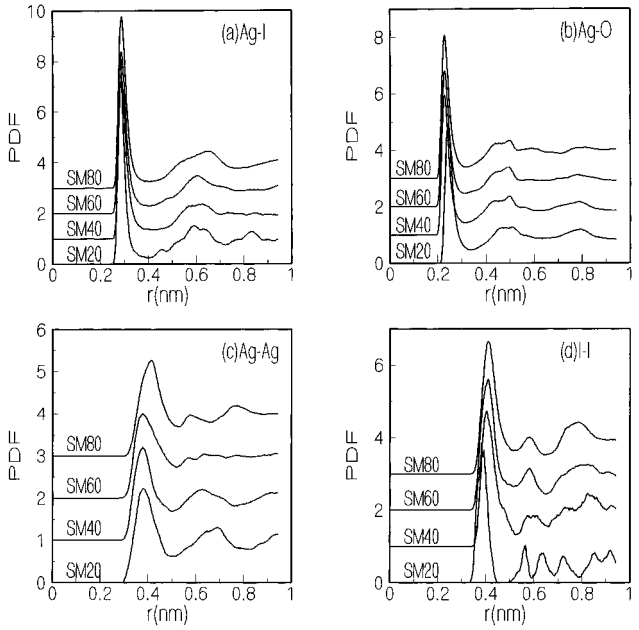

Figure 2. (a) Ag−I, (b) Ag−O, (c) Ag−Ag, and (d) I−I pair distribution functions at room temperature (300 K)for various compositions of glasses.

plot of molar cohesive energy of the system versus AgI composition is shown in Figure 1. From the figure it can be seen that the extrapolated value of the molar cohesive energy of pure AgI coincides with the molar cohesive energy value theoretically calculated by Ladd and Lee,[50] who used the Born−Mayer−Huggins model of ionic potentials. We have also plotted molar volumes from the model calculations. The extrapolated molar volume of (hypothetical) Ag_2MoO_4 glass is 63.0 cm^3 which is 3.5% higher than that of crystalline Ag_2MoO_4. On the other hand, the extrapolated molar volume of glassy AgI (36.0 cm^3) is about 7.7% lower than that of α-AgI. These fits as well as the good conservation of total cohesive energy of the system suggest that the present model potential (BMH) represents the real interactions satisfactorily.

3.1. Glass Structures. 3.1.1. Pair Correlation Functions. Three different pair distribution functions (PDFs) based on silver ions and one on iodide ion for various compositions of the glass at room temperature (300 K) are shown in Figure 2a−d. These represent data averaged for 60 ps in each case. The relevant features of the local structure around silver ions, namely, peak distances, coordination number, and cutoff distances, employed for calculating the coordination numbers are summarized in Table 3. The PDF of Ag−I exhibits a sharp first peak at about 2.87 Å. This Ag−I interaction distance agrees well with the experimental value of 2.87 Å found in EXAFS and X-ray RDF studies.[51] The iodine coordination number of Ag^+ increases

TABLE 3: Summary of Static Structure Data at 300 K Obtained from PDFs[a]

pair	composition AgI%	first peak position (Å)	coordination number	cutoff distance for coordination (Å)	second peak position (Å)
Ag−I	20	2.875	0.73(6.11)	4.075	5.875
	40	2.875	1.56(6.00)	4.225	6.125
	60	2.875	2.62(5.89)	4.175	6.050
	80	2.900	3.83(5.76)	4.100	6.550
Ag−O	20	2.425	6.23(2.43)	3.400	5.100
	40	2.275	4.22(1.80)	3.125	4.975
	60	2.275	3.24(1.45)	3.175	4.925
	80	2.275	1.86(1.43)	3.200	4.975
Ag−Ag	20	3.800	10.05	5.150	
	40	3.775	10.02	5.225	
	60	3.775	10.20	5.200	
	80	4.125	10.74	5.300	
Ag−Mo	20	3.125	4.52(10.19)	4.850	6.725
	40	3.525	3.44(9.15)	4.500	6.475
	60	3.400	2.39(9.06)	4.550	6.450
	80	3.500	1.43(8.79)	4.475	6.475
I−I	20	3.825	1.43	4.575	5.625
	40	4.025	2.08	5.250	5.775
	60	4.075	4.94	5.175	5.825
	80	4.100	7.68	5.200	5.825
I−O	20	3.475	11.56	4.575	5.375
	40	3.750	11.51	4.750	6.200
	60	3.675	08.57	4.825	6.075
	80	3.650	04.56	4.850	6.200
I−Mo	20	4.050	6.03	5.475	
	40	4.100	6.20	5.725	
	60	4.200	5.09	6.100	
	80	4.025	3.50	6.300	
Mo−O*	20	4.625	20.39	5.525	
	40	4.600	17.20	5.600	
	60	4.600	12.94	5.625	
	80	4.675	08.07	5.725	
O−O*	20	3.250	8.99	4.100	5.800
	40	3.325	8.65	4.275	5.725
	60	3.300	6.84	4.250	5.750
	80	3.325	5.03	4.300	5.875

[a] Asterisked values refer to PDFs between two different MoO_4^{2-} units. Numbers in parentheses are the reverse coordination numbers.

with AgI content in the glass. As shown in Table 3, in SM80 glass (80% of AgI) the iodine coordination number is 3.83 and is as high as in α-AgI structure,[52] if oxygen atoms are not considered.

Oxygen atoms are also present as first neighbors of Ag^+ ions in the glasses. Ag−O distances are expectedly shorter. In the AgI poor compositions Ag−O distances have a slightly greater spread and the peak distance is also slightly higher (2.425 Å) than in AgI rich glasses (2.275 Å). This is reflected in the first minimum distance in the respective PDFs which gradually decrease, and correspondingly the Ag−O peak appears narrower in AgI rich compositions. The spread in Ag−O distances in AgI poor glasses also correlates with the increased O/Ag ratio (SM20, O/Ag $\approx$ 1.8; SM80, O/Ag $\approx$ 0.6). At high O/Ag ratios more than one oxygen presumably seeks coordination to the same Ag^+ ion (like $Ag\langle_O^O$ rather than Ag−O), increasing the average Ag−O distance. This may be the situation in SM20 glass. There is a sharp decrease in the oxygen coordination numbers around Ag^+ ions from 6.2 in SM20 to 1.9 in SM80 with a corresponding increase in iodine coordination. It is interesting to note that while total first neighbor coordination ($n_O + n_I$) changes from 6.96 in SM20 to 5.69 in SM80, total Coulombic charge of the first neighbors decrease from 5.61 to 5.32 (electron) units. This has the effect of reducing the depth of the Coulombic well for the Ag^+ ion and thereby making it easy for it to migrate from one well to another. Thus AgI rich compositions are, as expected, more conducting.

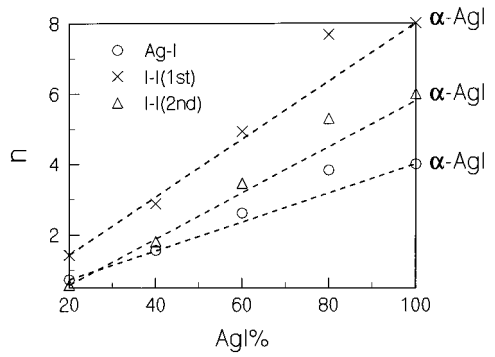

Figure 3. Plot of coordination numbers as a function of AgI content. The coordination values quoted for α-AgI correspond to bcc structure.

The second shell around Ag^+ ions is constituted of silver and molybdenum ions. The Ag−Ag PDF is shown in Figure 2c. Ag−Ag distances remain almost constant (3.775−3.800 Å) in the first three compositions (SM20 to SM60) but increase to 4.125 Å in SM80. It is remarkable, however, that the Ag−Ag coordination number is constant to within 7%, while AgI varies from 20 to 80 mol %, and actual molar concentration of Ag^+ ions in the glass decreases by one-third (form 1.8 to 1.2 mol by Ag^+ ions). This increase of AgI content is accompanied by a corresponding decrease in the oxygen coordination number around Ag^+ ions. The notable feature is the existence of some "motif" of Ag^+ ion arrangement in the glasses which is responsible for the near constancy of Ag−Ag coordination numbers. The Ag−Mo coordination number (Table 3) decreases expectedly from 4.52 to 1.43 in a manner somewhat similar to Ag−O coordinations, but the Ag−Mo coordination number is always less than the Ag−O coordination number, confirming that Ag^+ is coordinated to more than one oxygen ion of the same MoO_4^{2-} ion. Whenever more than one oxygen of the same MoO_4^{2-} is coordinated to Ag^+ ion, the Ag−Mo distance decreases, as reflected in Table 3. However, Ag−O distances of 1.89 Å reported in an earlier experiment[51] are not observed in this simulation. Some of the complementary coordinations such as I−Ag and Mo−Ag given in Table 3 are also interesting. I−Ag coordination is roughly 6 throughout the compositions. Despite a decrease in Ag^+ ion concentration, Mo−Ag coordination decreases marginally by less than 15% from SM20 to SM80; the coordination numbers are also high and similar to Ag−Ag coordinations. Of the several other pair distributions examined I−I pair distribution suggests a rapid increase in the coordination number toward SM80.

The I−I PDF is shown in Figure 2d. From Table 3 it can be seen that while I−I nearest coordination number for SM80 is 7.68, the second nearest neighbor coordination number is found to be 4.81. It is tempting to associate these two values of I−I coordinations to those in α-AgI structure, which is, however, not correct, as shown below. In Figure 3 a plot is shown of different coordination numbers for Ag−I (first coordination) and I−I (first and second) correlations as a function of AgI content in the glass. The distribution of Ag^+ and I^- ions in glass would be expected to vary linearly if there was no aggregate formation (preferential groupings) and would extrapolate to values characteristic of pure AgI, as indicated by dotted lines for each case. But the iodine coordination numbers obtained from the simulation exhibit significant positive deviation from linearity, particularly above 40% AgI. This indicates that some kind of ordering begins to appear above 40% AgI in the glass. However the ordered arrangement may not correspond to α-AgI structure, because the I−I peak positions in Figure 2d are not in agreement with such structure. The first I−I distance around 4.1 Å is comparable to the I−I bond

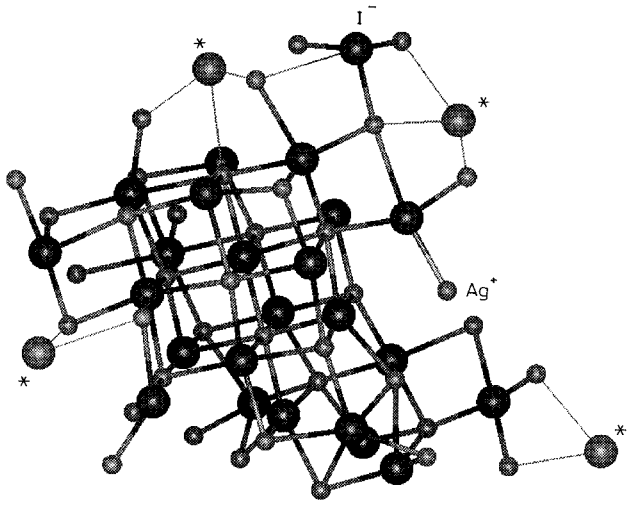

Figure 4. Snapshot of the atomic configuration in a small region of SM80 composition at 300 K. The asterisks represent the sites occupied by MoO_4^{2-} ions.

distances obtained from experiments (4.25 Å) but is much lower than its value in α-AgI (4.4 Å). If iodine atoms were arranged in an α-AgI-like framework (bcc), the second I−I neighbors have to be at 5.1 Å. However, the second I−I peak appears at 5.8 Å, and this distance is exactly equal to $\sqrt{2} \times 4.1$ Å (the first peak distance). The third (shoulder) and the fourth peak appear at 7.2 and 8.1 Å, respectively, which are approximately $\sqrt{3} \times 4.1$ and 2×4.1 Å, respectively. The arrangement of I^- ions appears more like a simple cubic lattice. A similar observation was also made by M. C. Abramo et al.[38] in their molecular dynamics simulation of $AgI-Ag_2O-B_2O_3$ glasses.

The AgI peak distance 2.875 Å is nearly half of the second I−I peak distance at 5.8 Å. Also, the Ag−Ag PDF in SM80 has a coordination number of 10.74 (after the first peak) and 19.05 (after the second peak), and these values are close to 12 and 18, respectively, which are expected for a fcc arrangement. A close analysis of the various other peak positions and coordination numbers suggests the formation of a distorted NaCl type of structure for the silver and iodide ions. This is also consistent with the I−Ag coordination number of 5.76, close to the expected 6 for octahedral sites. The I−I coordination number expected for such an arrangement is 12, but the observed value is only 7.68. This may be due to the fact that the tetrahedral MoO_4^{2-} anions whose radius (≈3.0 Å) is slightly greater than the iodide anion (2.2 Å) occupy iodide ion sites. This radius of MoO_4^{2-} ion was estimated by adding the effective radius of O^{2-} ion (1.22 Å) (Table 1) to the Mo−O distance (1.75 Å). The Mo−O distance is taken from experimental studies.[48] Further, the molar volumes of equilibrated model systems compare well with the known experimental molar volumes of crystalline AgI (39.0 cm^3) and Ag_2MoO_4 (60.8 cm^3). The unrealistically low value of the thermodynamic radius[2] of MoO_4^{2-} (2.54 Å) was therefore not favored in this work. Hence, when the coordination at I−Mo, which is equal to 3.5, is added to I−I coordination (7.68), the total coordination becomes 11.2, which is close to the expected value, 12. A snapshot of a small region that is dominantly AgI composition is shown in Figure 4. The fcc type of ordering present in the region is clearly evident. In the figure, the MoO_4^{2-} units occupying iodide ion "sites" are marked by asterisks ("sites" or "positions" here have the restricted meaning that they are anion positions occupied exclusively by either I^- or MoO_4^{2-} ions within these small clusters by virtue of coulombic interactions). A similar kind of structural arrangement is also observed in SM60 (with 60% of AgI), but with a greater number of I^-

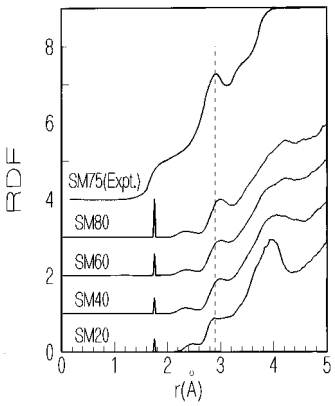

Figure 5. Total X-ray radial distribution function (RDF) for the simulated glasses. The experimental RDF of SM75 glass[51] is given for comparison.

ions substituted by molybdate units and thus with greater distortion of the structure. But in glasses containing less than 60% AgI, no ordering has been observed. Formation of small "clustered" regions of AgI is seen in AgI rich glasses typically consisting of four to six unit cells in all directions in SM80.

As noted earlier, the Mo−Ag correlations have a coordination number around 10 in all glasses. Similarly, an almost constant coordination number is observed for Ag−Ag and I−Ag pairs, together implying more or less a constant motif in the distribution of silver ions independent of composition and the Ag^+-Ag^+ interaction being one of strong Coulombic repulsion. The I−Mo and Mo−Mo PDFs (not presented) have a very broad first coordination peak, which is characteristic of the glass structure. The Mo−O PDF between two different molybdate units has a first peak at around 4.6 Å. The oxygen coordination number of Mo from these second neighbor MoO_4^{2-} units for SM20 glass is as high as 20.39, indicating that at least six to seven MoO_4^{2-} units are found around each MoO_4^{2-} unit. In the AgI rich SM80 this decreases to three MoO_4^{2-} tetrahedral units. The coordination number for the I−Mo PDF appearing at around 4.1 Å is about 6.0 up to 40% of AgI, and thereafter it falls to 3.5 in SM80. A similar observation of constancy (up to SM40) and a drop in coordination number toward SM80 is seen in I−O coordinations (refer to Table 3). This indicates that the ordering of iodide ion matrix builds up only above 40% of AgI in the glass, as noted earlier in the Ag−I and I−I coordinations. The O−O PDF between two different MoO_4^{2-} units has a first peak around 3.3 Å, and its coordination number decreases with AgI content in the glass. A comparison of O−O distances suggests that Ag^+ ions are likely to be present between tetrahedral MoO_4^{2-} units although not giving rise to linear O−Ag−O type geometries. This is inferred from the fact that the O−O distance (3.3 Å) is higher than twice the oxygen ion radius (1.22 Å) and less than the sum of the two oxygen radii plus the radius of Ag^+ ion (1.16 Å).

3.1.2. Radial Distribution Function. The radial distribution functions (RDFs) of the glasses have been calculated by convoluting all the PDFs, giving proper weight to their atomic scattering factors and mole fractions. The RDFs of the various glasses are presented in Figure 5. The narrow peak at 1.75 Å is due to the Mo−O distance in the rigid MoO_4^{2-} ion. The dominant peak at 2.87 Å and its shoulder at 2.27 Å one due to Ag−I and Ag−O distances, respectively. The experimental RDF for the SM75 glass reported in the literature[51] is given for comparison in Figure 5. It is seen that positions of major peaks observed experimentally for SM75 and in our simulation for SM80 compare satisfactorily. But we wish to point out that the origin of the peaks suggested in the work of Rajalakshmi et al.[51] and our assignments are different. Thus various structural features of the computer-simulated glass presented here for SM80 are in good agreement with experimentally observed features. The potential model and the various parameters employed for the simulation may therefore be considered satisfactory and realistic.

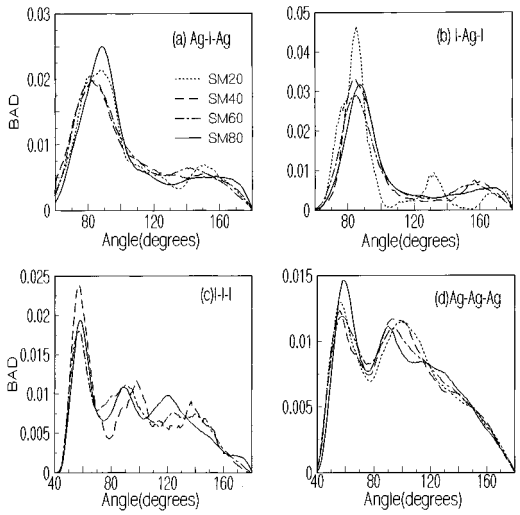

Figure 6. Bond angle distribution at room temperature (300 K) as a function of AgI composition in the glass for (a) Ag−I−Ag, (b) I−Ag−I, (c) I−I−I, and (d) Ag−Ag−Ag.

3.1.3. Bond Angle Distribution. The equilibrated structure of the glasses studied here have been further examined by calculating the bond angle distributions (BADs) at room temperature (300 K). The Ag−I−Ag and I−Ag−I bond angle distributions are shown in Figure 6a,b, respectively. Both Ag−I−Ag and I−Ag−I show a prominent peak at around 90°, as one would expect for a NaCl type of structure. This shows that the silver ions occupy the six-coordinated octahedral sites. The additional feature observed at around 160° in both parts a and b of Figure 6 can be attributed to the collinear arrangement of Ag−I−Ag ions and I−Ag−I ions, respectively, along the distorted cube edge; a perfect arrangement would lead to a 180° peak. Such distortions are evident from the snapshot picture shown in Figure 4. The I−I−I BADs shown in Figure 6c have well-resolved peaks at 60° and 90° and at 120° in the case of SM80. This is again consistent with the expected angles for a NaCl type of structure. The peak at 120° is not observed for AgI content below 60%; instead the second peak shifts toward higher angles and broadens. The type of ordering referred to above is unlikely to be present in glasses with less than 40% AgI. The Ag−Ag−Ag BAD also gives peaks at 60°, 90°, and 120° (clearly for SM80), indicating the octahedral nature of Ag^+ ion sites (see Figure 6d). Thus AgI clusters with NaCl-like cubic arrangement are observed in $AgI-Ag_2MoO_4$ glass at higher AgI contents. The O−Ag−O bond angle peaks at around 70° and thereafter decreases toward zero at 180° with some features around 90° and 120−130°. Since it involves oxygen both within the same MoO_4^{2-} units and from different MoO_4^{2-} units, the BAD of O−Ag−O is somewhat less informative. If the O−Ag distance (Table 3) is 2.3 Å, then the 70° angle suggests that Ag^+ ion is possibly sitting in contact with two oxygen atoms of the different MoO_4^{2-} units, because the calculated O−O distance in the $Ag\langle_O^O$ triangle ($=2 \times 2.3 \sin 35° \approx 2.6$ Å) is approximately equal to the sum of the radii of O^{2-} ions (2×1.22 Å $= 2.44$ Å).

3.1.4. Environment of Silver Ions. It has been suggested that the Ag^+ ions have two different anionic environment,[10,18] namely, glasslike (Ag^+ bonded to O^-) and saltlike (Ag^+ bonded

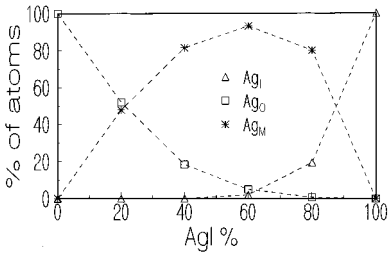

Figure 7. Plot of percentage of silver ions in different anionic environments. Ag_I^+, Ag_O^+, and Ag_M^+ represent silver ions surrounded by iodide, oxide, and a mixture of iodide−oxide ions, respectively.

to I^-). To know the anion population around each silver ion, an estimate of the number of iodide and oxide ions surrounding each Ag^+ ion has been calculated. The calculation represents averaging over 60 ps in all the compositions studied at 300 K. To differentiate the silver ions in different anionic environments, we have classified the Ag^+ ions as (i) completely surrounded by iodine anions and denoted as Ag_I^+ (i.e. well within the AgI clustered region), (ii) completely surrounded by oxygen anion, Ag_O^+, and (iii) surrounded by a combination of iodide and oxide ions, Ag_M^+. The percentages of Ag^+ ions in the three classes are shown in Figure 7 as a function of AgI content. It is seen that as the AgI content in the glass increases, the percentage of silver ions fully surrounded by iodide ions (Ag_I^+) increases from zero to 20%, while that for silver ions surrounded completely by oxygen ions (Ag_O^+) falls from 50% to zero. The percentage of silver ions with mixed oxygen−iodine coordination (Ag_M^+) increases with AgI content in the glass and reaches values as high as 90% in SM60. Only above 60% AgI in the glass composition do Ag^+ ions completely coordinated to iodide ions appear to become noticeable; correspondingly, a decreasing trend in the concentration of Ag_M^+ may be noticed. Some numbers are interesting. At 60% AgI, the ratio of I^-/MoO_4^{2-} ions is 1.5 and increases to 4.0 at 80% AgI. The ratio of I^-/Ag^+ increases from 0.43 to 0.66 in this region, where a significant increase of Ag_I^+ ions is seen. But in the same region the ratio of $([I^-] + [O^{2-}])/[Ag^+]$ decreases from 1.57 to 1.33. If we consider that 20% of the Ag_I^+ ions represent 20% AgI "clusters", the volume fraction of such clusters is roughly $[0.2 \times 39.0]/[(0.8 \times 39.0) + (0.2 \times 60.8)]$ (molar volumes of AgI and Ag_2MoO_4 are 39.0 and 60.8 cm^3, respectively), or 0.18. This points to the fact that percolation of AgI regions has already set in. The ratio reaches a value of 0.16 even around 65% AgI. The extrapolations in Figure 7 suggest that a steep increase in AgI-like regions would ensure above 80% AgI at the expense of Ag_M^+ in the glass structure. We will discuss in the next section dynamical properties obtained in this simulation that reveal the details of silver ion motion and the anion environment of silver ions.

3.2. Dynamical Properties. The dynamical properties of the glasses and the silver ion transport are examined by studying the velocity autocorrelation functions, mean square displacements, etc. For this purpose the coordinates (including those of quaternions) and velocities of the particles were stored for at least 60 ps at intervals of 10 fs, and the dynamical properties were evaluated from such stored data.

3.2.1. Velocity Autocorrelation Functions and Spectral Densities. The velocity autocorrelation functions (VAFs) of Ag^+ and I^- ions at 300 K have been computed for all compositions of the glasses. VAFs of Ag^+ ions in SM20 and SM80 are shown Figure 8a as examples. For both Ag^+ and I^- ions correlations extend to negative regions, indicating back-scattering of the ions. The VAFs indicate that there is a rapid

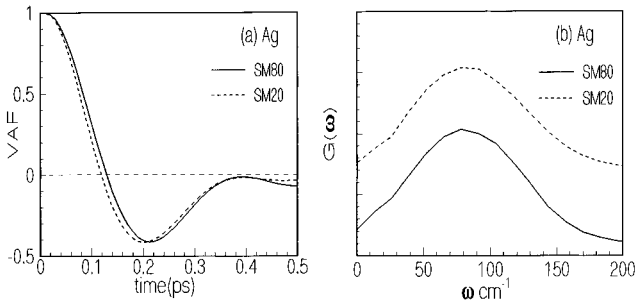

Figure 8. (a) Velocity autocorrelation function (VAF) and (b) power spectra of the silver ions in SM80 and SM20 glass compositions.

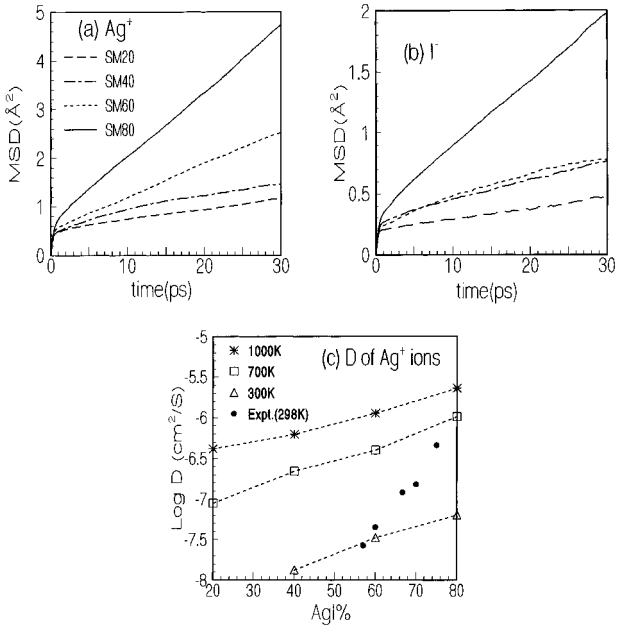

Figure 9. Mean square displacement (MSD) data for (a) silver and (b) iodide ions at 1000 K for various glasses. (c) Variation of the diffusion coefficient (D) of the silver ion as a function of AgI content at different temperatures. (The experimental D values are obtained from conductivity data[49] using the Nernest−Einstein relation.)

loss of memory (under 0.4 ps) and oscillations do not extend to longer times. There does not seem to be any pronounced coupling in the motions of Ag^+ and I^- ions. The corresponding power spectra have been calculated from the Fourier transforms of VAFs. The $G(\omega)$ provides information about cage-rattling frequencies. The $G(\omega)$ values for Ag^+ and I^- ions have also been examined in all cases. The variations are small, and $G(\omega)$ values of Ag^+ ions in SM20 and SM80 only are shown in Figure 8b. The smoothened peaks appear broad, and the peak frequencies (cage-rattling frequency) fall in the far infrared region. The vibrational frequencies peak around 85 cm^{-1} in the AgI rich glasses. This is very close to the vibrational frequency (110 cm^{-1}) observed in Raman experiments in pure AgI[53] and in Raman studies of $AgI-AgPO_3$ glasses.[54] In AgI poor glasses (40% and below), the Ag^+ ion vibration shifts slightly toward higher frequencies. This may be due to introduction of more oxygen ions in the cage surrounding Ag^+ ions (via MoO_4^{2-} ions). Introduction of more oxygen (in low AgI glasses as noted earlier in section 3.1.1) results in a slight increase in the net negative charge on the first-neighbor cage.

3.2.2. Mean Square Displacements. The mean square displacements (MSDs) of all the ions were computed, and those of Ag^+ and I^- ions in all compositions are presented in Figure 9a,b at 1000 K. We may note that the fictive temperatures of the computer quenched glasses are very high.[45] We could not, however, determine the T_g by the use of Abraham−Wendt

ratios since a clear change of slope could not be identified in any of the PDFs. In Figure 9a it is evident that the MSD values of Ag^+ ions increase with AgI content in the glass. The compositional dependence of the diffusion coefficient (D) of the silver ions calculated from MSD data is shown in Figure 9c for all three temperatures for which data were collected. Diffusion coefficients (and hence the conductivities) increase at all temperatures as the AgI concentration increases. The values of D calculated from the experimental conductivity data at 298 K (using Nernest−Einstein relation) are also shown in Figure 9c. In the case of SM60 glass the values from experiment (298 K) and simulation (300 K) agree very well. But the experimental values of D of the glasses increase much more rapidly with AgI concentration than suggested by the simulation. This renders the agreement between the experiment and simulation poor for other compositions. Since the MSD values of both I^- (Figure 9b) and MoO_4^{2-} (not presented) ions are rather low compared to the MSD of Ag^+ ions even at 1000 K, the corresponding diffusion coefficients of the two ions are an order of magnitude lower than that of Ag^+ ion. Therefore both I^- and MoO_4^{2-} ions can be considered as immobile and the simulated systems can be assumed to be in the glassy state even at 1000 K. With such high fictive temperatures the simulated glasses yield diffusion constants that can only be in qualitative agreement with the experimental values of D estimated using the Nernest−Einstein relation. Even then it was gratifying to note a reasonable comparison in magnitudes of diffusion coefficients. The detailed microscopic dynamics of the Ag^+ ions is considered in the following section.

3.2.3. Pathways for Silver Ion Motion. As mentioned earlier in section 3.1.4, silver ions are distributed in different anionic environments to different extents in different compositions of glasses. Indeed Minami and co-workers[10] had thoughtfully postulated the existence of two distinct populations of silver ions, although their emphasis has been on their mobilities. It was suggested that a "mobile" silver ion population was associated with I^- ions and an "immobile" silver ion population was linked with oxy-anionic species in the glasses. However the NMR investigations[16] were inconclusive, and the postulate of different types of Ag^+ ions with different migration properties could not be supported. In the present work we have already identified in section 3.1.4 three different populations of Ag^+ ions. It is therefore possible to evaluate the MSD of the three classes of silver ions, namely, Ag_I^+, Ag_O^+, and Ag_M^+. The jumps of silver ions from one class of anionic environment to another are carefully eliminated while evaluating MSDs of individual classes of Ag^+ ions.

The MSDs of these three class of silver ions for various compositions of glasses at 1000 K are shown in Figure 10a−c. It may be noted that the mobility of Ag_M^+ is the highest even in the glass with 80% AgI. In SM20 and SM40 (see Figure 10c), the Ag_I^+ population is so low that no meaningful (poor statistics) MSD calculations could be performed. However the MSD value in Ag_O^+ is close to the MSD of Ag_M^+ in SM20, and the MSD of Ag_O^+ decreases as AgI concentration increases. The individual contributions of the three silver ion species to the total conductivity are plotted in Figure 10d. These were calculated on the assumption of conductivity additivity and using the Nernest−Einstein relation. It is seen that in the entire composition range the contribution of Ag_M^+ ion is the highest. Even in the glass with 80% AgI, Ag_I^+ contribution is close to a tenth of the total conductivity. The contribution of Ag_O^+ to the total conductivity is throughout marginal. Thus insofar as dc conductivity is concerned, only the Ag_M^+ type of silver ions seems to be important, and these ions possess mixed iodide−

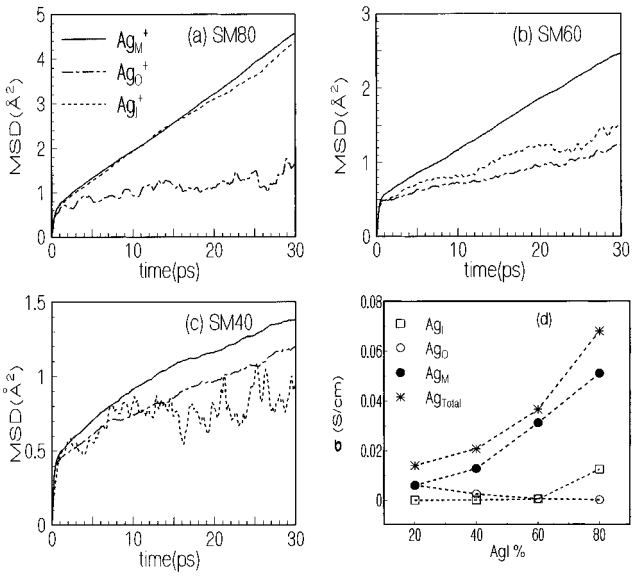

Figure 10. Mean square displacement for the different types of silver ions at 1000 K in various glass compositions: (a) SM80, (b) SM60, and (c) SM40. (d) Conductivity of silver ions in different anionic environments at 1000 K as a function AgI in the glass. Ag_{Total} corresponds to conductivity of all the silver ions considered as a single class.

oxide (molybdate ion) coordination. In SM20, Ag_O^+ ions have an MSD comparable to the Ag_M^+ ions. This is a consequence of their increased population (see Figure 7), and hence they would naturally form long connected paths. By the same argument we feel that the Ag_M^+ class of silver ions contributes the most to the MSD due to the fact that their path lengths and connectivities are always more than either Ag_I^+ or Ag_O^+ ions.

The time-dependent pair correlation functions provide further insight regarding migration paths of Ag^+ ions. To do this, we have calculated the Van Hove correlation function,[45] $G_d^{ij}(r,t)$ (the distinct part of the Van Hove correlation function). First we have considered the general case where all the silver ions are treated equally, and then we go on to the particular case of silver ions in different anionic environments.

3.2.4. Van Hove Correlation Function. The distinct part of the Van Hove correlation function is defined as

$$G_d^{ij}(r,t) = (1/N)\langle \sum_i^N \sum_{j\neq i}^N \delta[\vec{r} + \vec{r}_i(0) - \vec{r}_j(t)]\rangle \qquad (2)$$

i and j sites are fixed in space during computation and denote positions occupied by the indicated ions at $t = 0$. $G_d^{ij}(r,t)$ is averaged over all individual migrations. First, we have employed $G_d^{ij}(r,t)$ to study the nature of migration of Ag^+ to a site of its own type $\overline{Ag}$.[55] In fact we wish to call $\overline{Ag}$ a silver ion vacancy because $Ag \rightarrow \overline{Ag}$ can occur only when a site occupied by Ag^+ ion is vacated by the occupant and such a vacant site possesses an unbalanced charge of opposite sign; the repulsive interactions arising from the previous occupant ceases to exist and the unbalanced charge switches on monopole-induced dipole (and other successively weaker multipole) interactions.[56] Figure 11 shows $G_d^{ij}(r,t)$ curves for four different compositions of the glass at 1000 K for different times. The gradual buildup of $G(r,t)$ close to the origin as a function of time with a simultaneous drop in the intensity of the curve at peak position is observed only in AgI rich glasses (Figure 11a,b). This can be interpreted as follows: The reference silver ion i moves out of its own site and the i site becomes a vacancy. Its neighboring ion j also moves out of its position in a similar

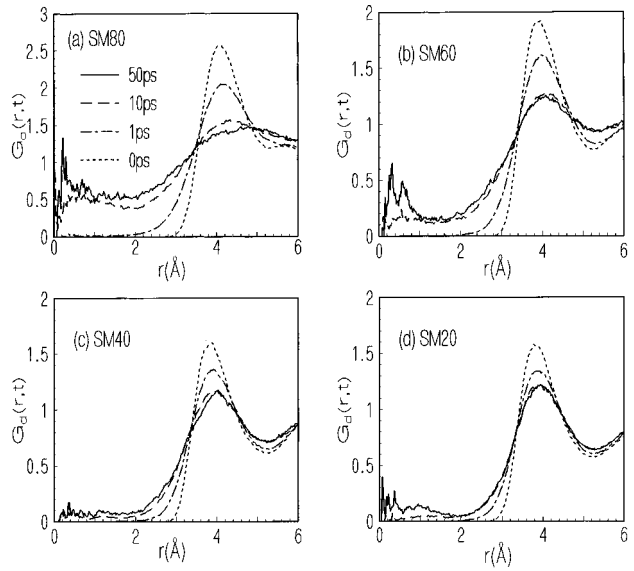

Figure 11. $G_d(r,t)$ plotted as a function of distance at four different times for Ag^+ ion migration to neighboring Ag^+ ion vacancy sites in glasses; (a) SM80, (b) SM60, (c) SM40, and (d) SM20.

manner. The loss at the *j* ion site is observed as a decrease in intensity and broadening of the peak. However some of the *j* ions move into the vacancy created by the reference ion *i*. This is observed as a buildup of $G(r,t)$ close to the origin. The $G(r,t)$ develops peaks around 0.1−0.2 Å but not at the origin as expected. This is due to a shift in the reference site itself owing to the structural relaxation in the local environment. However a buildup of $G(r,t)$ is observed between the origin and *j* ion positions, which smears out the peaklike character at *i*, suggesting substantial relaxation at 1000 K over time scales of 50 ps.

In the AgI poor glasses the buildup of $G(r,t)$ around the origin is not significant, although there is an observable loss of intensity of the 4.0 Å peak, suggesting either (i) several positions similar to *i* ion position are available around the *j* ion in MoO_4^{2-} rich structure (these are potential Ag^+ ion sites around MoO_4^{2-} ions which are possibly numerically many more than around I^- ion) or (ii) jump times are longer. We have seen earlier that the mobilities (Figure 9) are not greatly affected by composition in the case of the model glass (although the conductivity variation with composition observed experimentally is much higher), and therefore we feel that the presence of similar sites around Ag^+ ion is responsible for the observed phenomena. However, careful examination of Figure 11 suggests that the number of ions that move out of their sites in the 50 ps period is significantly higher in AgI rich glasses than in AgI poor glasses (loss of intensity at 4.0 Å peak), which is a likely consequence of increased connectivities (paths generated by continuous connection of equivalent sites) in AgI rich glasses. Similar results were obtained at 700 and 300 K also.

3.2.5. Jump Events of Silver Ions. The site equivalence implies an equivalence of the coordination sphere (its composition) as a minimum criterion. Ag_I^+ position is therefore equivalent to another Ag_I^+ ion position but not to Ag_O^+ or Ag_M^+ sites (in fact Ag_M^+ ions have a spread in the composition of coordination spheres around them; *m* oxides and *n* iodides where both *m* and *n* vary but $m + n \approx 6$ (see Table 3)). We now examine the $G_d^{ij}(r,t)$ of the three kinds of Ag^+ ions, namely, Ag_I^+, Ag_O^+, and Ag_M^+. The $G(r,t)$ for these silver ions to like and unlike sites are calculated for the glasses at 1000 K. In Figure 12a,b the $G(r,t)$ for the jump events to like ion sites are shown respectively for $\overline{Ag_M^+} \leftarrow Ag_M^+$ and $\overline{Ag_I^+} \leftarrow Ag_I^+$ in the

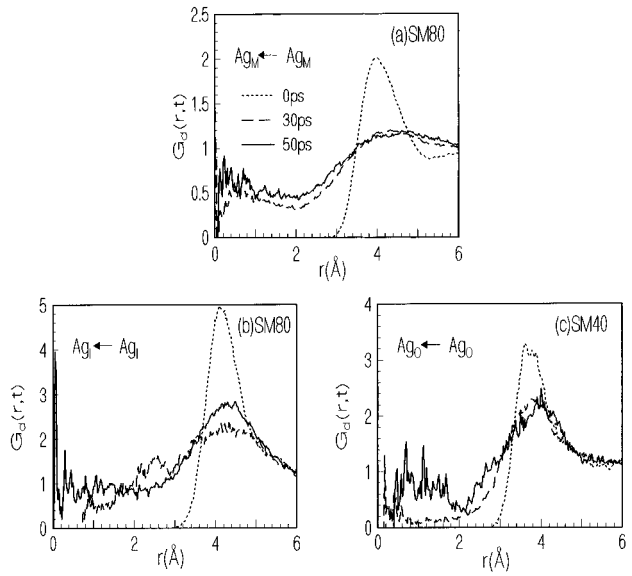

Figure 12. $G_d(r,t)$ plotted as a function of distance at three different times for like ion sites: (a) Ag_M^+ ion migration to neighboring Ag_M^+ ion vacancy site in SM80, (b)Ag_I^+ to Ag_I^+ ion vacancy in SM80, and (c) Ag_O^+ to Ag_O^+ ion vacancy in SM40.

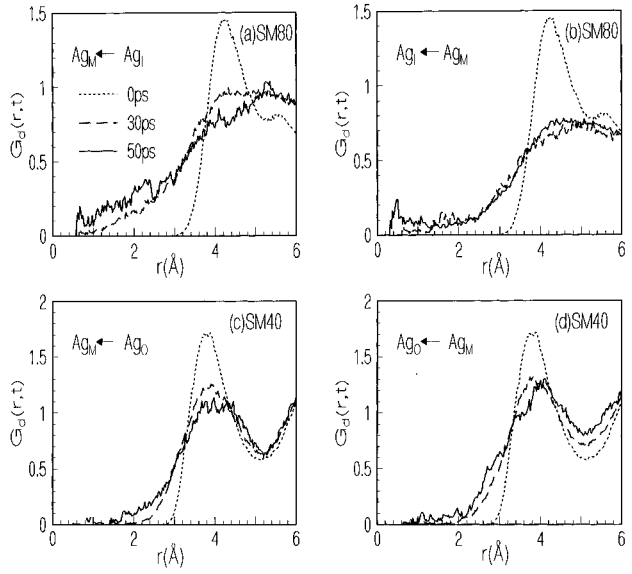

Figure 13. $G_d(r,t)$ plotted as a function of distance at three different times for unlike ion sites: (a) Ag_I^+ ion migration to neighboring Ag_M^+ ion vacancy site in SM80, (b) Ag_M^+ to Ag_I^+ ion vacancy in SM80, (c) Ag_O^+ to Ag_M^+ ion vacancy in SM40, and (d) Ag_M^+ to Ag_O^+ ion vacancy in SM40.

case of SM80 glass. In Figure 12c we have shown $G(r,t)$ for $\overline{Ag_O^+} \leftarrow Ag_O^+$ jumps in SM40 glass (this is because we have better averaging for $\overline{Ag_O^+} \leftarrow Ag_O^+$ in $Ag_2\,MoO_4$ rich glass). All these $G(r,t)$'s suggest the growth of peaks near the origin, indicating jumps occurring between sites of the same ion type (like ion sites). Similar results have been obtained for other glass compositions.

The jump events involving different types (unlike) of ion sites, $\overline{Ag_M^+} \leftarrow Ag_I^+$, $\overline{Ag_I^+} \leftarrow Ag_M^+$, $\overline{Ag_M^+} \leftarrow Ag_O^+$, and $\overline{Ag_O^+} \leftarrow Ag_M^+$, are shown in Figure 13a−d, respectively. From this figure it can be seen that there is hardly any buildup of intensity near the origin, although loss of intensity of the peak at 4.1 Å is very evident. This indicates that jumps to unlike ion sites are generally not preferred. The preferential jumps to like ion sites have an important consequence to Ag^+ ion conductivity in this

TABLE 4: Percolation Paths among Silver Ions and the Step Distances

type of silver ion	are the paths connected in the glass?			
	SM20	SM40	SM60	SM80
Ag_I^+	no	no	no	yes 4.5 Å
Ag_O^+	yes 4.6 Å	no	no	no
Ag_M^+	yes 4.4 Å	yes 4.1 Å	yes 3.9 Å	yes 3.9 Å

class of glasses, because the main factor that decides the long-range migration of silver ions is their path connectivity through like ion sites. The range of such path connectivities is expected to be short for Ag_I^+ and Ag_O^+ ion sites, as seen from their statistics, and thus their contribution to migration is limited. The connectivity among Ag_M^+ sites dominates in all glasses studied here, and it is responsible for the transport of Ag^+ ions. To quantify such path connectivities, we have examined whether there exists any percolation path for silver ion migration in the following section.

3.2.6. Percolation Paths for Silver Ions. The distribution of silver ions in different anionic environments is shown in Figure 7. For all three classes of silver ions we have examined if there exist any percolation paths in any or all directions. The jump distances for such paths are taken as roughly the Ag−Ag distances found in the PDFs. The results are tabulated in Table 4 for the three types of silver ions. Ag_I^+ sites do not show any percolation paths even in SM60 (60% AgI in the glass). Only in SM80 are connected paths of Ag_I^+ ions (jump distance 4.5 Å) seen. Formation of such paths is consistent with the closeness of MSD of Ag_I^+ and Ag_M^+ ions in Figure 10a. In all other compositions where such paths do not seem to exist the MSD of Ag_I^+ ions is much less than that of Ag_M^+ ions. Similar observations are true in the case of Ag_O^+ ions. In 20% AgI glass, the percolation paths for Ag_O^+ ions exist albeit with a jump distance of 4.6 Å, which is slightly higher than the Ag−Ag peak distance of 3.8 Å. The MSD values of Ag_O^+ ions are somewhat low compared to other types of silver ions in AgI dominant glasses. Nevertheless the percolation path is completed along Ag_O^+ sites in SM20, and it gives rise to a MSD of Ag_O^+ ions comparable to that of Ag_M^+ ions, as seen in section 3.2.3.

The Ag_M^+ ions exhibit percolation paths in all compositions. The minimum percolation distance for these ions comes out to be 3.9 Å, which is very close to the Ag−Ag peak distance obtained for these glasses. In the case of SM40 and SM20, however, the percolation distance is slightly greater than the Ag−Ag distance. For the 20% AgI glass the percolation paths appear only at 4.4 Å, well above the Ag−Ag peak distance of 3.8 Å. The increase in percolation distance indicates the reduction in jump events and thus the conductivity. The existence of a percolation path along Ag_M^+ sites confirms that the migration of silver ions occurs largely only along these paths in all compositions of the glasses. This is also evident from the dominating MSD of Ag_M^+ ions in Figure 10.

3.2.7. Energetics of the Ion Sites. The presence of preferential jumps to like ion sites is a very curious observation. To ascertain if the observed migration is related to the energetics of the silver ion sites, we have evaluated Ag^+ site ion energies for the three types of Ag^+ ions in their minimum energy configurations. The Ag_I^+ ion site energies are found to be higher than Ag_M^+ site energies in glasses with 60% and more of AgI. Even then $\overline{Ag_M^+} \leftarrow Ag_I^+$ jumps have not been significant.

TABLE 5: Attempt (ν_0) and Jump (ν) Frequency and Corresponding Activation Energy (E_ν)[a]

glass	ν_0	ν	E_ν (eV)	E_σ (eV)	E_a (eV)
SM20	2.3×10^{12}	3.50×10^{10}	0.35	0.31	0.36
SM40	2.3×10^{12}	3.45×10^{10}	0.36	0.21	0.33
SM60	2.9×10^{12}	3.76×10^{10}	0.37	0.21	0.28
SM80	2.9×10^{12}	3.73×10^{10}	0.37	0.15	0.21

[a] The activation energy obtained from conductivity plots of the simulation are listed as E_σ. In the last column experimental values of E_a are given.

Similarly in AgI poor glasses, jumps between Ag_O^+ sites (higher energy) and Ag_M^+ sites have also not been seen. Therefore the energy gain resulting from ion jumps into low-energy sites does not seem to be important. It is also evident that coupled jumps (like simultaneous $\overline{Ag_M^+} \leftarrow Ag_I^+$; $\overline{Ag_I^+} \leftarrow Ag_M^+$) are also not likely. Thus in an equilibrated $AgI-Ag_2MoO_4$ glass there are three classes of sites (and correspondingly three classes of vacancies), and ionic motions occur independently among the three types of paths created by them. It would be natural to expect in such situations a phenomenon similar to the mixed alkali effect to occur. But the absence of such a conductivity anomaly in our glasses is likely to be due to a preponderance of Ag_M^+ sites for which (a) the connectivity of paths is not broken in the entire composition range (see Table 4) and (b) their contribution to conductivity is always the highest. However this important observation requires further investigation.

3.2.8. Jump Time and Activation Energy. The jump time distribution, i.e. the time between any two jumps, has been calculated for all compositions of the glasses at 1000 K. The jump distances for these calculations are taken around the Ag−Ag pair distance. The distribution (not shown) is found to be somewhat shapeless for AgI poor glasses, while it is more bell shaped in AgI rich glasses. The first moment of this distribution $\int_0^{t_{max}} t\ f(t)\ dt$ gives the average jump time. The attempt frequency may be taken as the cage vibrational frequency, ν_0, obtained from the Fourier transform of the velocity autocorrelation function. The activation energy for conduction can then be evaluated using the expression $E_a = RT \ln(\nu_0/\nu)$. The activation energy values obtained in this manner (Table 5) range from 0.35 to 0.37 eV, which is somewhat higher than the experimental values. The activation barriers examined this way are also not very sensitive to composition. The activation barriers were also evaluated by directly plotting model conductivities and the temperatures in Arrehenius plots. These activation barriers are listed in Table 5, but these values were obtained on the basis of just two temperatures. The E_a values obtained in conductivity experiments have also been included in Table 5 for comparison.

4. Conclusions

The silver molybdate glasses examined in this molecular dynamics simulation work exhibit various structural features in good agreement with experimental observations. It is found that, in AgI rich glasses, silver and iodide ions form aggregates. It is interesting that these regions exhibit a sodium chloride structure rather than that of α-AgI. The vibrational frequency of the simulated glasses in clustered domains is close to the frequency observed in pure AgI. The conductivity increases as a function of silver halide content and is consistent with experiments. The Ag^+ ion conductivity in compositions relevant to known experimental studies seems to occur largely through percolation of Ag^+ ions in the paths created by Ag_M^+ ion sites that have mixed iodide−oxide coordinations. A rather surpris-

ing observation has been that there is a preference in ion jumps that occur among sites of like type. Formation of percolation paths with an iodide ion environment is significant only above 80% AgI in the glasses.

References and Notes

(1) Ingram, M. D. *Phys. Chem. Glasses* **1987**, *28*, 215.
(2) Minami, T.; Katsuda, T.; Tanaka, M. *J. Non. Cryst. Solids* **1978**, *29*, 389.
(3) Tachez, M.; Mercier, R.; Malugani, J. P.; Chiuex, P. *Solid State Ionics* **1987**, *25*, 263.
(4) Minami, T. In *Materials for solid state batteries*, Chowdari, B. V. R.; Radhakrishna, S.; Ed., World Scientific, 1986; p 181.
(5) Minami, T.; Imazawa, K.; Tanaka, M. *J. Non. Cryst. Solids* **1980**, *42*, 469.
(6) Tachez, M.; Mercier, R.; Malugani, J. P.; Dianoux, A. P. *Solid State Ionics* **1986**, *20*, 93.
(7) Rousselot, C.; Tachez, M.; Malugani, J. P.; Mercier, R.; Chiuex, P. *Solid State Ionics* **1991**, *41*, 151.
(8) Owens, B. B.; Starstad, P. M.; Underekar, D. F. In *Hand book of batteries and fuel cells*, David Linden; Ed.; Mc Graw Hill, New York, 1984.
(9) Angell, C. A. *Solid State Ionics* **1986**, *18* and *19*, 72.
(10) Minami, T. *J. Non. Cryst. Solids* **1985**, *73*, 273.
(11) Ingram, M. D.; Mackenzie, M. A.; Muller, W.; Torge. *Solid State* Ionics **1988**, *28*−*30*, 677.
(12) Rao, K. J.; Wong, J.; Hemlata, S. *Proc. Indian Acad. Sci. (Chem. Sci.)* **1985**, *94*, 449.
(13) Dalba, G.; Fornasini, P.; Rocca, F. *J. Non. Cryst. Solids* **1990**, *123*, 310.
(14) Malugani, J. P.; Mercier, R.; Tachez, M. *Solid State Ionics* **1986**, *21*, 131.
(15) Carini, G.; Cutroni, M.; Federico, M.; Tripodo, G. *Solid State* Ionics **1986**, *18* and *19*, 415.
(16) Martin, S. W.; Bischof, H. J.; Mali, M.; Roos, J.; Brinkmann, D. *Solid State Ionics* **1986**, *18* and *19*, 421.
(17) Villa, M.; Chiodelli, G.; Magistris, A.; Licheri, G. *J. Chem. Phys.* **1986**, *85*, 2392.
(18) Kamitsos, E. I.; Kapoutsis, J. A.; Chryssikos, G. D.; Hutchinson, J. M.; Pappin, A. J.; Ingram, M. D.; Duffy, J. A. *Phys. Chem. Glasses* **1995**, *36*, 141.
(19) Shiraldi, A.; Pizzati, E.; Baldini, P.; Martin, S. W. *Solid State Ionics* **1986**, *18* and *19*, 426.
(20) Malugani, J. P.; Wasniewski, Doreau, M.; Robert, G.; Mercier, R. *Mater. Res. Bull.* **1978**, *13*, 1009.
(21) Borjesson, L.; Torell, L. M.; Howells, W. S. *Phil. Mag.* **1989**, *B59*, 105.
(22) Musinu, A.; Paschina, G.; Piccaluga, G.; Pinna, G. *Solid State Ionics* **1989**, *34*, 187.
(23) Musinu, A.; Piccaluga, G.; Pinna, G. *J. Non. Cryst. Solids* **1988**, *10*, 70.
(24) Musinu, A.; Piccaluga, G.; Pinna, G. *J. Chem. Phys.* **1988**, *89*, 1074.
(25) Dalba, G.; Fornasini, P.; Fontana, A.; Rocca, F.; Borattini, E. *Solid State Ionics* **1988**, *28*−*30*, 713.
(26) Tatsumisago, M.; Shinkuma, Y.; Saito, T.; Minami, T. *Solid State Ionics* **1992**, *50*, 273.
(27) Tatsumisago, M.; Shinkuma, Y.; Minami, T. *Nature* **1991**, *354*, 217.
(28) Rao, K. J.; Rao, C. N. R. *Mater. Res. Bull.* **1982**, *17*, 1337.
(29) Rao, K. J. *Proc. Indian Acad. Sci. (Chem. Sci.)* **1984**, *93*, 389.
(30) Senapati, H.; Parthasarathy, G.; Lakshmikumar, S. T.; Rao, K. J. *Phil. Mag.* **1983**, *B47*, 291.
(31) Hemlata, S.; Parthasarathy, G.; Rao, K. J.; Gopal, E. S. R. *Pramana* **1984**, *23*, L269.
(32) Ingram, M. D.; Mackenzie, M. A.; Muller, W.; Torge. *Solid State Ionics* **1990**, *40* and *41*, 671.
(33) Schiraldi, A. *Electrochim. Acta* **1978**, *23*, 1039.
(34) Mercier, R.; Malugani, J. P.; Tachez, M.; Dianoux, A. J.; Rousselot, C. *Acad. Sci. Paris Ser. II* **1986**, *303*, 345.
(35) Fontana, A.; Rocca, F.; Fontana, M. P. *Phy. Rev. Lett.* **1987**, *58*, 503.
(36) Dianoux, A. J.; Tachez, M.; Mercier, R.; Malugani, J. P. *J. Non. Cryst. Solids* **1991**, *131*−*133*, 973.
(37) Abramo, M. C.; Pizzimenti, G.; Consolo, A. *Phil. Mag.* **1991**, *64*, 495.
(38) Abramo, M. C.; Caccamoand, C.; Pizzimenti, G. *J. Phys. Condens. Matter* **1993**, *5*, 397.
(39) Wicks, J. D.; Borjesson, L.; Bushnell-Wye, G.; Howells, W. S.; McGreevy, R. L. *Phys. Rev. Lett.* **1995**, *74*, 726.
(40) Soules, J. F. *J. Non. Cryst. Solids* **1982**, *49*, 29.
(41) Soules, J. F. *J. Non. Cryst. Solids* **1990**, *123*, 48.
(42) Damodaran, K. V.; Rao, B. G.; Rao, K. J. *Phys. Chem. Glasses* **1990**, *31*, 212.
(43) Damodaran, K. V.; Nagarajan, V. S.; Rao, K. J. *J. Non. Cryst. Solids* **1990**, *124*, 233.
(44) Balasubramanian, S.; Rao, K. J. *J. Phys. Chem.* **1993**, *97*, 8835.
(45) Balasubramanian, S.; Rao, K. J. *J. Non. Cryst. Solids* **1994**, *181*, 157.
(46) Rao, K. J.; Balasubramanian, S.; Damodaran, K. V. *J. Solid State Chem.* **1993**, *106*, 174.
(47) Allen, M. P.; Tildesly, D. J. *Computer Simulations of Liquids*; Clarendon: Oxford, 1987.
(48) Wilson, A. J. C. *Struct. Rep.* **1951**, *11*, 291.
(49) Minami, T.; Tanaka, M. *J. Solid State Chem.* **1980**, *32*, 51.
(50) Ladd, M. F. C.; Lee, W. H. *J. Inorg. Nucl. Chem.* **1959**, *11*, 264.
(51) Rajalakshmi, A.; Seshasayee, M.; Aravamudan, G.; Yamaguchi, T.; Nomura, M.; Ohtaki, H. *J. Phys. Soc. Jpn.* **1990**, *59*, 1252.
(52) Vashista, P.; Rahman, A. *Phys. Rev. Lett.* **1978**, *40*, 1337.
(53) Burns, G.; Dacol, F. H.; Schafar, M. W. *Solid State Commun.* **1976**, *19*, 291.
(54) Rao, K. J.; Shastry, M. C. R. *Spectrochim. Acta* **1990**, *46A*, 1581.
(55) Bunde, A.; Ingram, M. D.; Maass, P.; Ngai, K. L. *J. Non. Cryst. Solids* **1991**, *131*−*133*, 1109.

(56) Notations like $\overline{Ag}$, etc., were first used by Bunde et al.[55] and subsequently by us specifically in molecular dynamics calculations related to mixed alkali effect.[44,45] Path connectivity in relation to alkali ion motion has also been similarly used in the references above.